Volume and fat infiltration of spino-pelvic musculature in adults with spinal deformity

Bertrand Moal, Nicolas Bronsard, José G Raya, Jean Marc Vital, Frank Schwab, Wafa Skalli, Virginie Lafage

Bertrand Moal, Frank Schwab, Virginie Lafage, Spine Division, Hospital for Joint Diseases, New-York University University Langone Medical Center, New York, NY 10003, United States

Nicolas Bronsard, Nice University Hospital Center, Orthopedic and Traumatologic Surgery Department, Hôpital Saint Roch, 06000 Nice, France

José G Raya, Center for Biomedical Imaging, Department of Radiology, New York University Langone Medical Center, New York, NY 10016, United States

Jean Marc Vital, University Hospital of Bordeaux, Spinal Unit, Departement of Orthopaedic Surgery, 33000 Bordeaux, France

Wafa Skalli, Laboratory of Biomechanics, Arts et Métiers ParisTech, 75013 Paris, France

Author contributions: All authors contributed equally to this work.

Supported by International Spine Study Group and ParisTech BiomecAM chair program on subject-specific musculoskeletal modeling, with the support of Proteor, Covea, Société Général, ParisTech and Yves Cotrel Foundation.

Institutional review board statement: Institutional review board approval.

Clinical trial registration statement: This study is registered at New York University of Medicine's Institutional Review Board. The registration identification number is 11-01647.

Informed consent statement: All study participants, or their legal guardian, provided informed written consent prior to study enrollment.

Conflict-of-interest statement: Bertrand Moal, Nicolas Bronsard, José G. Raya and Jean Marc Vital have no conflicts of interest to declare; Frank J. Schwab is a consultant and received grants for research purpose by Medtronic and Depuy. He is a shareholder of Nemaris. Wafa Skalli has royalties from EOS imaging (Royalties) and received a grant for research purpose by the Fondation ParisTech chair program on subject specific musculoskeletal modelling. Virginie Lafage received a grant for research purpose by SRS and ISSG. She is giving lectures for Globus, Depuy Spine, Medtronic, Nuvasive and MDT. She is a shareholder of Nemaris.

Data sharing statement: Technical appendix, statistical code, and dataset available from the corresponding author at Virginie.lafage@gmail.com. Consent from participants was not obtained but the presented data are anonymized and risk of identification is low.

Correspondence to: Virginie Lafage, PhD, Spine Division, Hospital for Joint Diseases, New-York University University Langone Medical Center, 306 E. 15th St., New York, NY 10003, United States. virginie.lafage@gmail.com
Telephone: +1-646-7948646
Fax: +1-646-6026926

Abstract

AIM: To investigate fat infiltration and volume of spino-pelvic muscles in adults spinal deformity (ASD) with magnetic resonance imaging (MRI) and 3D

reconstructions.

METHODS: Nineteen female ASD patients (mean age 60 ± 13) were included prospectively and consecutively and had T1-weighted Turbo Spin Echo sequence MRIs with Dixon method from the proximal tibia up to T12 vertebra. The Dixon method permitted to evaluate the proportion of fat inside each muscle (fat-water ratio). In order to investigate the accuracy of the Dixon method for estimating fat *vs* water, the same MRI acquisition was performed on phantoms of four vials composed of different proportion of fat *vs* water. With Muscl'X software, 3D reconstructions of 17 muscles or group of muscles were obtained identifying the muscle's contour on a limited number of axial images [Deformation of parametric specific objects (DPSO) Method]. Musclar volume (Vmuscle), infiltrated fat volume (Vfat) and percentage of fat infiltration [Pfat, calculated as follow: Pfat = 100 × (Vfat/Vmuscle)] were characterized by extensor or flexor function respectively for the spine, hip and knee and theirs relationship with demographic data were investigated.

RESULTS: Phantom acquisition demonstrated a non linear relation between Dixon fat-water ratio and the real fat-water ratio. In order to correct the Dixon fat-water ratio, the non linear relation was approximated with a polynomial function of degree three using the phantom acquisition. On average, Pfat was 13.3% ± 5.3%. Muscles from the spinal extensor group had a Pfat significantly greater than the other muscles groups, and the largest variability (Pfat = 31.9% ± 13.8%, $P < 0.001$). Muscles from the hip extensor group ranked 2nd in terms of Pfat (14% ± 8%), and were significantly greater than those of the knee extensor ($P = 0.030$). Muscles from the knee extensor group demonstrated the least Pfat (12% ± 8%). They were also the only group with a significant correlation between Vmuscle and Pfat ($r = -0.741$, $P < 0.001$), however this correlation was lacking in the other groups. No correlation was found between the Vmuscle total and age or body mass index. Except for the spine flexors, Pfat was correlated with age. Vmuscle and Vfat distributions demonstrated that muscular degeneration impacted the spinal extensors most.

CONCLUSION: Mechanisms of fat infiltration are not similar among the muscle groups. Degeneration impacted the spinal and hip extensors most, key muscles of the sagittal alignment.

Key words: Spino-pelvic musculature; Adults with spinal deformity; Muscular degeneration; Muscular volume; Fat infiltration; Dixon method

Core tip: Volume and fat infiltration of spine, hip, and knee extensor and flexor muscles of 19 patients with spinal deformity were evaluated with an innovative method combining dedicated magnetic resonance imaging acquisition (Dixon method) and 3D reconstructions. The results demonstrated that mechanisms of fat infiltration are not similar among the muscle groups. Degeneration impacted the spinal and hip extensors most, key muscles of the sagittal alignment, highlighting the need for considering muscular factors beyond skeletal parameters.

Moal B, Bronsard N, Raya JG, Vital JM, Schwab F, Skalli W, Lafage V. Volume and fat infiltration of spino-pelvic musculature in adults with spinal deformity. *World J Orthop* 2015; 6(9): 727-737 Available from: URL: http://www.wjgnet.com/2218-5836/full/v6/i9/727.htm DOI: http://dx.doi.org/10.5312/wjo.v6.i9.727

INTRODUCTION

The muscular system plays an essential role in the maintenance of postural balance, however, there has only been limited investigation into the relationship between the muscular system and structural alignment pathologies.

In adult spinal deformity (ASD), recent research has highlighted the critical role of sagittal spino-pelvic alignment in patient-reported pain and function[1-4]. Therefore, key muscles involved in pelvic-positioning and lumbar-stabilization are at the forefront of research needs.

Preliminary efforts have been directed towards understanding spine or thigh muscles using histological analyses[5-8], muscular strength[9-12], electromyographical signals[13-15], muscle cross-sectional areas [via ultrasound, computed tomography (CT)-scan or magnetic resonance imaging (MRI)][11,15-26], measurement of muscular density with CT-scan[15-18,27], or muscular intensity with MRI[10,11,22,23,25,26,28]. However, difficulties arise in representing inter-muscle and inter-subject variability[29].

To overcome these limitations, Jolivet *et al*[30-32] developed a method of three-dimensional muscle reconstruction *via* segmentation of a few axial images (MRI or CT-scan). This method has been successfully implemented with CT scans for analysis of muscles involved in knee motion[33] and hip muscles[34]. Nevertheless, the radiation exposure from CT scans makes it unacceptable as a tool for studies involving ASD patients, frequently subjected to radiographic examination. Notably, the method has also been performed using MRI sequences[33]. However, contrary to CT scans, MRI cannot be interpreted in terms of tissue composition, so quantification of fat and muscle requires the use of dedicated MRI pulse sequences.

Dixon *et al*[35-40] developed a MRI method for fat quantification which exploits the slight difference in the Larmor frequency of fat and water protons (chemical shift). By acquiring the signal at different echo times,

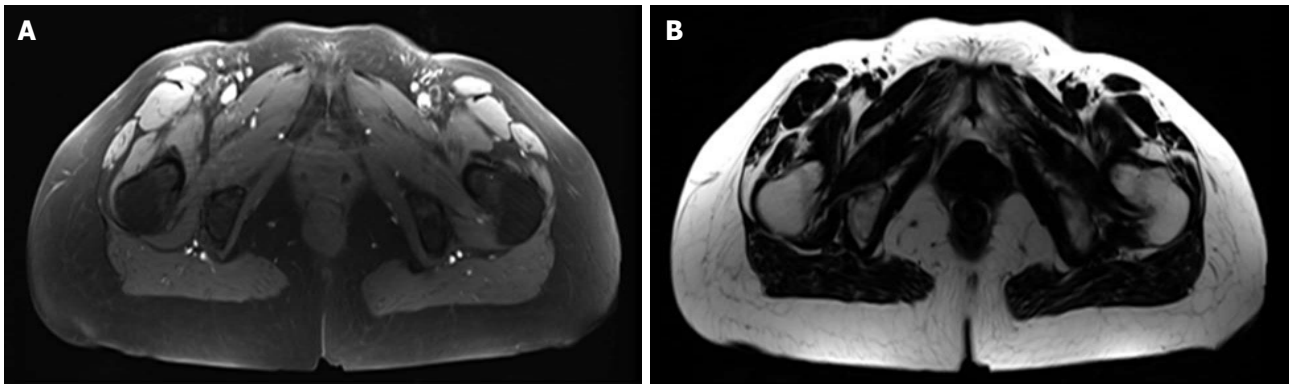

Figure 1 Example of water (A) and fat (B) images with Dixon methods on a 64-year-old female adult spinal deformity patient.

the modulation of the signal intensity can be fitted and the fat and water content can be separated.

Thus, by utilizing Dixon acquisitions and 3D muscular reconstructions, muscular volume and fat infiltration has been obtained and used to investigate the main functional groups of muscles associated with sagittal posture. The hypothesis is that volume loss and fat infiltration, previously demonstrated as factors of skeletal muscle degeneration due to aging[41,42], do not equally affect the different muscles.

MATERIALS AND METHODS

Inclusion/exclusion criteria

This study is a prospective consecutive pilot series of ASD patients, recruited following international review board approval and written informed consent. Inclusion criteria were female patients over 35 years old and at least one of the following radiographic parameters: Thoraco-lumbar or lumbar coronal Cobb angle greater than 30°, sagittal vertical axis (SVA) greater than 4 cm, or pelvic tilt (PT) greater than 20°. Patients with existing instrumentation, history of spine surgery, or presenting contraindication for MRI were excluded.

Radiographic acquisition and measurements

All patients underwent a full-length coronal and lateral X-ray in free standing position[43]. Radiographs were measured using a validated spine software[44,45] (SpineView, Laboratory of Biomechanics ENSAM ParisTech, France), which provided the following spino-pelvic parameters: Coronal plane: Cobb angle and apex location, coronal alignment; Sagittal plane: SVA, PT, pelvic incidence (PI), pelvic incidence minus lumbar lordosis (PI-LL), lumbar lordosis (L1S1), thoracic kyphosis (T4T12).

Patients MRI acquisition

MRI was performed on a 3T whole-body scanner (Magnetom Skyra, Siemens Healthcare, Erlangen, Germany) using a 24-channel spine matrix coil and three 16-channel flex coils from the same vendor. The imaging protocol included a T1-weighted Turbo Spin Echo sequence for applying the two point Dixon method[35-38] [Repetition time (TR)/Echo time = 820/11 ms, acquisition matrix = 448 × 308, phase oversampling = 100%, in plane resolution = 0.94 × 0.94 mm^2, 4 stages, 40 slices by stage, slice thickness = 5 mm, slice gap = 0 mm, flip angle = 157°, turbo factor = 3, echo trains = 107, parallel imaging acceleration factor (iPat) = 2, iPat references lines = 26, bandwidth = 319 Hz/pixel, echo spacing = 15.7, acquisition time per stage = 5:53 min, Total acquisition time = 25 min]. Water and fat images were automatically generated by the scanner from in and out of phase images (Figure 1). Imaging volume covered the proximal tibia to the lumbar spine (T12 vertebra) and was acquired in four stages.

Phantom MRI acquisition

In order to investigate the accuracy of the 2 points Dixon method for estimating fat *vs* water, the same MRI acquisition was performed on phantoms composed of four 10 mL plastic vials. One vial was filled with soybean oil (100% fat) and another full of water (0% fat). The remaining two vials contained an emulsion of 10% and 20% fat obtained from intralipid 20% fat emulsion (Sigma-Aldrich, St. Louis, MO, United States). For the acquisition, the phantoms were submerged in a phosphate buffered saline solution.

3D muscle reconstruction

The 3D reconstruction of individual muscles, listed Table 1, was performed using Muscl'X software (ENSAM, Laboratory of Biomechanics, Paris, France)[26,30,32,33]. The reconstruction technique is based on the deformation of parametric specific objects (DPSO algorithm) as described by Jolivet *et al*[30-32] and briefly summarized hereafter.

For each muscle, a subset of MRI axial slices (MSS: manually segmented slices) were manually segmented. These contours were then approximated by ellipses, and cubic spline interpolation was used to interpolate ellipses on each intermediate MRI slice. These interpolated ellipses were deformed non-linearly using the manual segmentations of MSS. All segmentations were then verified by the operator.

Table 1 Muscles analyzed in this study, and grouping by function and joint

	Spine extensor	Spine flexor	Hip extensor	Hip flexor	Knee extensor	Knee flexor	Total muscle
Quadratus lumborum	x						x
Tractus medialis	x						x
Tractus lateralis	x						x
Psoas		x		x			x
Iliacus		x		x			x
Biceps femoris short			x			x	x
Biceps femoris long			x			x	x
Semi-membranosus			x			x	x
Semi-tendinosus			x			x	x
Gluteus maximus			x				x
Rectus femoris				x	x		x
Gracilis				x		x	x
Sartorius				x		x	x
Adductor				x			x
Tensor fascia lata				x			x
Vastus lateralis intermedius					x		x
Vastus medialis					x		x

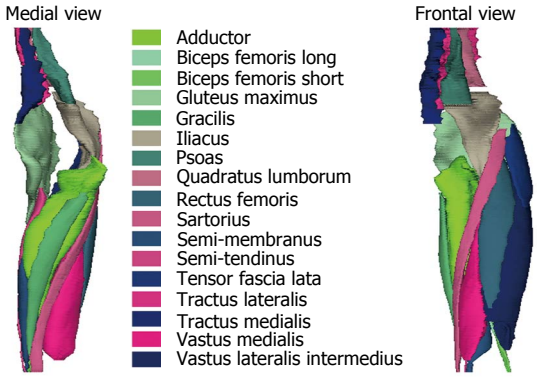

Figure 2 Medial and frontal view of all the left muscles reconstructed for one patient.

Some muscles were combined, since the low contrast made an accurate separation of the individual muscles difficult. The lumbar part of the psoas was reconstructed separately, but at a point where the distinction with the iliacus was not possible, it was then integrated into the iliacus. The external obturator, adductor longus, brevis and magnus and pectineus were reconstructed into a single group named "Adductor". The vastus lateralis and intermedius were reconstructed together. The muscle reconstructions were done on the fat images. Figure 2 presents the 3D reconstruction of the left muscles for one patient. The femurs were also reconstructed on the water images, the contrast between the cortical and cancellous bone was greater on water images.

Right and left muscles were grouped according to the joint (spine, hip, and knee) and by mechanical action (extensor/flexor) (Table 1). The entire set of muscles were also grouped and named total muscles.

Real fat water ratio: Correction from fat-water ratio with Dixon method

From the fat and water images, the fat-water ratio by voxel was calculated using equation 1 where SI_{fat} represents the signal intensity of the fat signal and SI_{water} the signal intensity of the water image:

$$\text{Dixon Dixon fat-water ratio} = 100 \times [SI_{fat}/(SI_{fat} + SI_{water})] \quad (1)$$

From the Phantom acquisition, an 8-by-10 region of interest (ROI) was drawn in the center of each vial and the mean and the standard deviation of the Dixon fat-water ratio in each ROI were then calculated. Those results demonstrated a non linear relation between Dixon fat-water ratio and the real fat-water ratio. In order to correct the Dixon fat-water ratio, the non linear relation was approximated with a polynomial function of degree three (F) using the phantom acquisition. Then for each patients, the real fat-water ratio was calculated for each voxel for with equation 2.

$$\text{Real fat-water ratio} = F(\text{Dixon fat-water ratio}) = 0.0002 \times (\text{Dixon fat-water ratio})^3 - 0.0071 \times (\text{Dixon fat-water ratio})^2 + 0.5607 \times (\text{Dixon fat-water ratio}) - 0.7714 \quad (2)$$

If F (Dixon fat-water ratio) was less than 0%, real fat-water ratio was evaluated at 0 and if F (Dixon fat-water ratio) was greater than 100, real fat-water ratio was evaluated at 100.

Quantification of fat components and muscle parameters

From the 3D reconstructions, muscular volumes were calculated (Vmuscle). The volume of infiltrated fat inside each muscles (Vfat) was calculated with the real fat-water ratio. The volumes were then normalized based upon the volume of the right femur, in an effort to limit the impact of the patient morphology. For each joint, the ratio of Vmuscle and Vfat between flexors and extensors were calculated. The percentage of fat infiltration (Pfat) was also expressed and was calculated as follow: Pfat = 100 × (Vfat/Vmuscle).

Statistical analysis

Muscular volumes and fat infiltration distribution were characterized as well as Pfat. Paired *t*-test was used

Table 2 Demographic information

	Min	Max	Mean	SD	95%CI	
					Lower	Upper
Age	37	80	60	13	54	66
BMI	17.4	31.2	22.9	3.52	21.1	24.6

BMI: Body mass index.

Table 3 Mean and standard deviation of Dixon fat-water ratio for the phantom with the different concentrations of fat

Vails	Real fat concentration (%)	Dixon fat-water ratio (%)
Only soybean oil	100	85.4 ± 0.3
Intralipid 20% fat emulsion	20	38.7 ± 1.7
Intralipid 10% fat emulsion	10	22.2 ± 1.0
Only water	0	1.4 ± 0.6

to compare muscular volumes and fat infiltration distribution and Anova *t*-tests were used to compare muscular groups. For the Anova test, an analysis of the homogeneity of variance was performed, followed by Bonferonni or Games-Howell tests. Pearson's correlation coefficient was used to investigate the relationship between muscle parameters and demographic data. For each statistical analysis, the level of significance was set at 0.05.

RESULTS

Demographics

19 consecutive ASD patients with a mean age of 60 years old (range: 37-80) and a mean body mass index (BMI) of 22.9 kg/m^2 (range 17.4-31.2) were included (Table 2). There was no significant correlation between age and BMI (r = 0.375, P = 0.114).

Radiographic analysis

In the coronal plane, the mean coronal alignment was 23 mm (range: 0-119 mm, 16% of the patients reached a threshold of 40 mm). The mean maximal Cobb angle was 40° (range: 0°-60°, 79% of the patients reached the threshold of 30°). Forty-seven percent of the patients had a double curve, 32% a single curve, and 21% did not exhibit any coronal curve.

Thoracic kyphosis ranged between -91° and -8° with average of -51° ± 22°. The mean L1S1 was 54° (range: 15°-75°) for a mean PI of 55° (range: 30°-77°). The analysis of PI-LL (mean = 1°, range = -35°-55°) revealed that 21% of the patients were above the threshold defined by the SRS-Schwab classification[3,46]. SVA ranged from -66 to 118 mm. The analysis of the PT revealed that 38% of the patients reached a threshold of 20°[3].

Phantom analysis and correction of the Dixon fat-water ratio

The Table 3 presented the mean and standard deviation of Dixon fat-water ratio for the phantom with the different concentrations of fat. As previously mentioned, the function F, presented in equation 2, was used to approximated this non linear relation between the Dixon fat-water ratio and the real fat-water ratio (Figure 3).

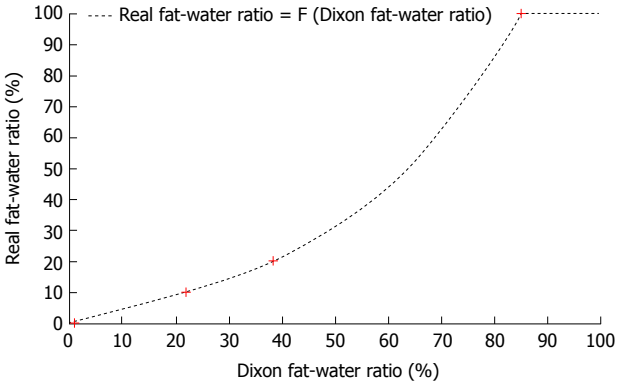

Figure 3 Average fat-water ratio for the phantom with different concentration of fat (0%, 10%, 20% and 100%) and the approximated function real fat-water ratio = F (Dixon fat-water ratio).

Muscle analysis

Femoral volume normalization: The average femoral volume was 414 ± 71 cm^3. A larger femoral volume was associated with a larger muscular volume when considering the Total Muscle (Pearson r^2 = 0.837, P-value < 0.001).

Muscle and fat infiltration repartition by functional groups: "Hip group" Vmuscle was significantly bigger than the "Knee group" Vmuscle which in turn was significantly bigger than those of the "Spine Group" (Figure 4 and Table 4). The Spine extensor group represented on average 9% ± 2% of the total muscular volume but a greater proportion (21% ± 7%) of the total infiltrated fat volume (P < 0.001). The hip extensor group represents 29% ± 2% of the total muscular volume and 32% ± 5% of the total infiltrated fat volume (P < 0.001). For the Spine extensor group and the knee extensor group, the distribution of muscular volume and infiltrated fat was similar (respectively 7% and 17% with standard deviation less than 2%). For the hip flexor and knee extensor groups the distribution of infiltrated fat was significantly smaller than the distribution of muscular volume (P < 0.001).

Percentage of fat infiltration: Pfat: The analysis of Pfat (Table 5) within each group of muscles revealed not only a large variability among patients (range: 6.1%-28.8%, Figures 5 and 6), but also highlighted the difference of Pfat between muscle groups. Muscles from the spinal extensor group had a Pfat significantly greater than the other muscles groups, and the largest variability (Pfat = 31.9% ± 13.8%, P < 0.001). Muscles from the hip extensor group ranked 2nd in terms of Pfat (14% ± 8%), and were significantly greater than those of the knee extensor (P = 0.030). Muscles from the knee extensor group demonstrated the least Pfat (12%

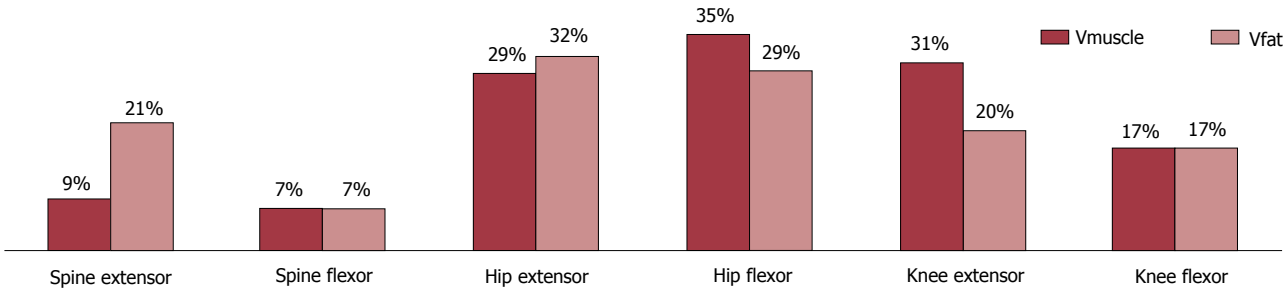

Figure 4 Distribution of Muscular volume and infiltrated fat volume expressed in percentage of the total muscle muscular volume and of the total infiltrated fat volume respectively. Vmuscle: Muscular volume; Vfat: Infiltrated fat volume.

Table 4 Muscular Volumes of each muscle group

	Muscular volume					
	Min	Max	Mean	SD	95%CI	
					Lower	Upper
Spine extensor	0.92	1.89	1.46	0.27	1.33	1.59
Spine flexor	0.85	1.67	1.24	0.22	1.13	1.34
Hip extensor	3.42	6.00	4.83	0.63	4.52	5.13
Hip flexor	4.79	7.13	5.91	0.71	5.57	6.25
Knee extensor	3.70	6.95	5.15	0.86	4.73	5.57
Knee flexor	2.18	3.41	2.88	0.33	2.72	3.04
Total muscles	12.87	19.44	16.67	1.87	15.77	17.57

Reported values are normalized based upon the volume of the right femur of each patient (for example, the mean "Total Muscles" volume = 16.67 femurs volume).

Table 5 Percentage of infiltrated fat expressed by functional groups

	Percentage of fat component					
	Min	Max	Mean	SD	95%CI	
					Lower	Upper
Spine extensor	12.72	71.15	31.90	13.83	25.24	38.57
Spine flexor	5.67	20.39	11.92	3.63	10.17	13.66
Hip extensor	6.39	38.09	14.81	7.01	11.43	18.19
Hip flexor	6.10	20.22	10.76	3.16	9.24	12.29
Knee extensor	3.84	20.02	8.66	4.03	6.72	10.60
Knee flexor	6.93	25.44	12.81	4.20	10.78	14.83
Total muscles	6.12	28.84	13.34	5.33	10.77	15.91

± 8%). They were also the only group with a significant correlation between Vmuscle and Pfat (r = -0.741, P < 0.001), however this correlation was lacking in the other groups.

Flexors *vs* extensor: The comparison of flexor *vs* extensors revealed a larger flexor contribution with regards to Vmuscle for the hip. For the spine, the ratio flex/ext highlight the greater fat infiltration of the extensor (Table 6).

Age *vs* muscle parameters (Table 7): No correlation was found between Vmuscle and age except for the knee extensors (Pearson's r = -0.701, P = 0.001). For Vfat, all groups were significantly and positively correlated with age (Pearson's r between 0.555 and 0.645) except the Spine groups. Except the spine extensor, Pfat was positively and significantly correlated with age.

BMI *vs* muscle parameters (Table 8): For the Spine groups, no correlation was found between Vmuscle, Vfat or Pfat and BMI. Vmuscle of the hip extensors and the knee flexors was significantly and positively correlated with BMI (respectively, Pearson's r = 0.642, P = 0.003 and Pearson's r = 0.470, P = 0.042). BMI was correlated with Vfat and Pfat in the hip and knee flexor and extensor.

DISCUSSION

While the radiographic presentation of ASD patients commonly demonstrates coronal and sagittal components of malalignment, sagittal spino-pelvic parameters have been identified as the main radiographic drivers of disability[2,47-49]. The objective of the current study was to investigate the volume and fat infiltration of the main functional groups of muscles associated with sagittal posture.

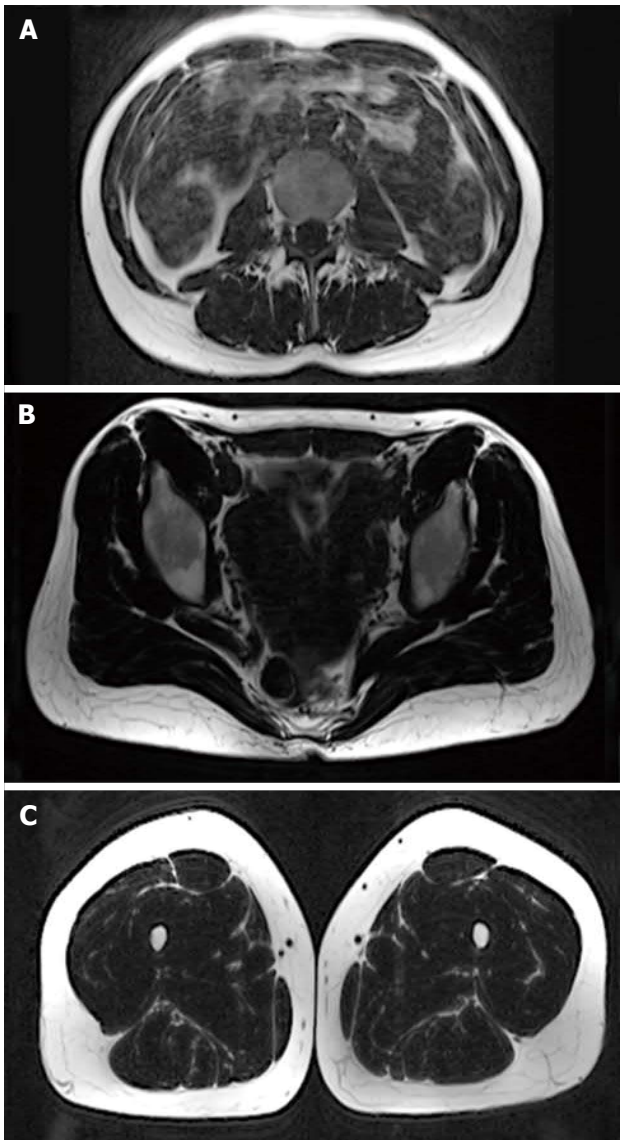

Figure 5 Magnetic resonance imaging samples (A: Lumbar area; B: Pelvis area; C: Limb area) of a 37-year-old female adult spinal deformity patient with a body mass index of 22 kg/m^2. This patient presents a sagittal deformity with hyperlordosis of the lumbar spine (pelvic incidence minus lumbar lordosis = -29°) and a thoraco-lumbar kyphosis of 45°. The analysis of the muscle quality revealed an 6.1% of fat infiltration on average.

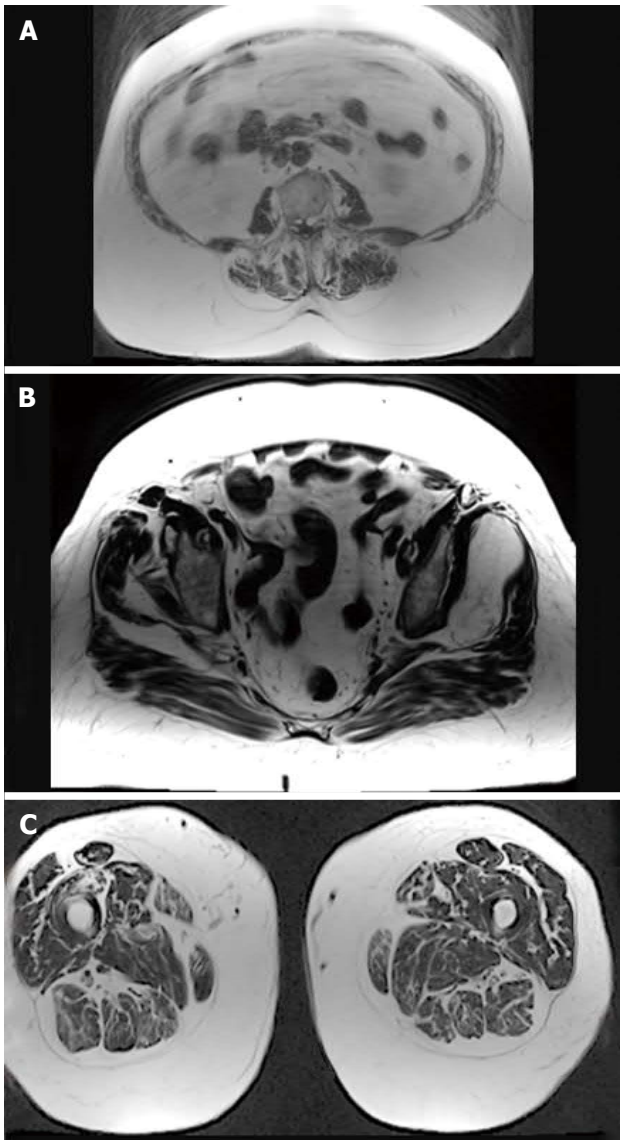

Figure 6 Magnetic resonance imaging samples (A: Lumbar area; B: Pelvis area; C: Limb area) of an 80-year-old female with a body mass index of 31 kg/m^2. This patient presents a degenerative scoliosis with a thoraco-lumbar Cobb angle of 32°, a hyperkyphosis of the thoracic spine (thoracic kyphosis = 63°) and a global sagittal malalignment (sagittal vertical axis = 11 cm). The analysis of the muscle quality revealed an 28.8% of fat infiltration on average.

Relationship with posture

Fat infiltration within muscle groups ranged from 8.7% and 31.9% on average-the least affected being the knee extensors. This suggests that muscular degeneration, evaluated with fat infiltration, does not impact the groups of muscles to the same extent. The lumbar spine extensors had the greatest percentage of fat component (31.9%). This is particularly interesting in regard to the loss of lumbar lordosis present in most ASD patients[4] because lumbar spine extensors are highly involved in the maintain of lumbar lordosis. Furthermore, correlations between fat infiltration and age for the spine were smaller than for the other groups and no correlation was found with the BMI. These results suggest that the greater degeneration of those muscles is probably not solely attributed to age and BMI. However the study cannot conclude whether this observation is a cause or a consequence of the spinal deformity.

Moreover, in the ASD population, sagittal malalignment is highly associated with pelvic retroversion, described by PT[1] and the agonist of this retroversion, the hip extensor, has the second greatest percentage of fat infiltration.

Flexor and extensor fat infiltration ratios were found to be smaller for the spine groups. This finding in the ASD population studied may reflect the unfavorable balance of forces leading to sagittal plane deformity across the trunk. Coupled with the findings of hip extensors and loss of contractile component with ageing, components of sagittal spino-pelvic misalignment from a perspective of soft tissue imbalance are emerging.

Table 6 Ratio between flexors and extensors for each group of muscles (muscular volume and infiltrated fat volume)

	Ratio flex/ext: Vmusle						Ratio flex/ext: Vfat					
	Min	Max	Mean	SD	95%CI		Min	Max	Mean	SD	95%CI	
					Lower	Upper					Lower	Upper
Spine	0.61	1.21	0.87	0.17	0.79	0.95	0.10	0.68	0.36	0.14	0.29	0.42
Hip	1.02	1.43	1.23	0.13	1.17	1.29	0.54	1.31	0.95	0.19	0.86	1.04
Knee	0.42	0.72	0.57	0.08	0.53	0.61	0.66	1.10	0.87	0.12	0.81	0.93

Vmuscle: Muscular volume; Vfat: Infiltrated fat volume.

Table 7 Correlation between age and muscular volume, infiltrated fat volume and percentage of fat component

		Vmuscle		Vfat		Pfat	
		r	*P*	*r*	*P*	*r*	*P*
Age	Spine extensor	-0.208	0.393	0.420	0.073	0.480[a]	0.038
	Spine flexor	-0.417	0.076	0.208	0.393	0.427	0.068
	Hip extensor	0.018	0.943	0.564[a]	0.012	0.633[b]	0.004
	Hip flexor	-0.309	0.198	0.555[a]	0.014	0.658[b]	0.002
	Knee extensor	-0.701[b]	0.001	0.645[b]	0.003	0.680[b]	0.001
	Knee flexor	-0.319	0.183	0.589[b]	0.008	0.679[b]	0.001
	All muscles	-0.433	0.064	0.614[b]	0.005	0.676[b]	0.001

Statistically significant difference with [a]*P*-value < 0.05; Statistically significant difference with [b]*P*-value < 0.01. Vmuscle: Muscular volume; Vfat: Infiltrated fat volume; Pfat: Percentage of fat component.

Table 8 Correlation between age and muscular volume, infiltrated fat volume and percentage of fat component

		Vmuscle		Vfat		Pfat	
		r	*P*	*r*	*P*	*r*	*P*
BMI	Spine extensor	0.127	0.606	0.017	0.944	-0.038	0.876
	Spine flexor	-0.027	0.913	0.443	0.057	0.450	0.053
	Hip extensor	0.642[b]	0.003	0.693[b]	0.001	0.587[b]	0.008
	Kip flexor	0.159	0.515	0.657[b]	0.002	0.587[b]	0.008
	Knee extensor	-0.236	0.330	0.596[b]	0.007	0.518[a]	0.023
	Knee flexor	0.470[a]	0.042	0.761[b]	< 0.001	0.570[a]	0.011
	All muscles	0.207	0.394	0.592[b]	0.008	0.458[a]	0.049

Statistically significant difference with [a]*P*-value < 0.05; Statistically significant difference with [b]*P*-value < 0.01. Vmuscle: Muscular volume; Vfat: Fat volume; Pfat: Percentage of fat component.

Fat infiltration, age and BMI

The difference between muscular volume and infiltrated fat volume demonstrated that muscle degeneration is not similar among the different functional groups. Those differences were highlighted by the difference of correlation between age and BMI. Only knee extensor muscular volume loss was correlated with age, however, infiltrated fat was correlated with age for each muscle group (except Spine Flexor $P = 0.068$), reflecting that age-related muscular degeneration is in general more associated with an increase of fat infiltration than an absolute muscular volume loss.

Greater BMI was associated with a greater percentage of infiltrated fat for hip and knee groups, but also associated for the hip extensor and the knee flexor groups with an increase of the muscular volume.

In light of the wide range of age and BMI values observed in this pilot study, the current findings will have to be confirmed in a larger population.

Fat and contractile component evaluation

The evaluation of the fat infiltration using the two points Dixon method has already been applied to investigate different organs (liver[38,40], bones[39] and muscles[36,50]). The decay in signal intensity between the in-phase and opposed phase images due to T2* was not taken into account[38]. The measurement of T2* would have required additional measurements or the use of sequences (*e.g.*, multi echo gradient echo sequences) that were not available at our scanner. Even more, the limited ability of patients with spinal deformities to hold still in the magnet forced us to reduce the scan time, so we could not measure T2* on these patients. Recent studies have shown that the two point Dixon without T2* has excellent concordance with spectroscopy measured in the spine, bones[39], liver[40], or spine muscles[50].

With the 3 points Dixon method applied onto phantoms filled with different proportions of fat and water, Kovanlikaya *et al*[51], demonstrated a linear

correlation between the fat-water ratio and the proportion of fat. However in our phantom study, this relationship was not linear, explaining why we corrected the fat water ratio evaluated with the two Dixon method with a polynomial function.

This disagreement observed between the nominal and the measured fat fraction in phantoms can be caused partially because of the T1 weighting of the images. Fat have much shorter T1 values (300 ms) than water in muscle (900 ms) at 3T[52]. With a TR of 820 ms the magnetization from fat was almost completely relaxed [TR/T1fat approximately 2.73, (1-e-TR/T1fat) = 0.94, *i.e.*, 94% of the signal available for the next excitation], while the magnetization for water did not have enough time to recover [TR/T1water approximately 0.91, (1-e-TR/T1water) = 0.60, *i.e.*, 60% of the signal available for the next excitation]. Therefore in our measurements the signal from water was underestimated and this resulted in overestimation of the fat fraction. Additional errors with the two-point Dixon included sensitivity to B0 inhomogeneity, which could explain why the differences between the in phase and out of phase in the 100% phantom lead to an underestimation of the fat fraction for large values of the fat fraction.

While investigations of the muscles of the thigh[36] or extensor of the spine[50] exist, they are based on a limited number of MRI slices and none of them report results on the entire muscular volume. To our knowledge, there is no study combining 3D reconstruction of muscles and fat component calculated with the two points Dixon method.

Limitations

Due to our experimental design and the limited sample size, we cannot draw any definitive conclusions correlating ASD and muscular factors. The various deformities presented in this population limited the ability to associate changes in a specific muscle groups with deformation type. Given the fact that the prevalence of adult spinal deformity is greater in female than in male patients, only female subjects were included in this study in an effort to limit confounding factors related to gender's difference in muscular system. Female subjects were considered due to the higher incidence of spinal deformity in the female population[6,20]. Data for a larger gender mixed population and an asymptomatic population are important next steps to evaluate more clearly the contractile component and correlation between muscle groups of the spino-pelvic complex and spino-pelvic alignment.

The applied MRI protocol permits a quantitative and qualitative characterization of the main muscles involved in the spino-pelvic complex. Regarding the differences between distribution of muscular and contractile components only, this study demonstrated the necessity of a complete characterization of the muscular system (including the quantification of the fat infiltration) and stress the limitations of considering only geometric parameters. Muscle degeneration seems more related to fat infiltration than volume loss but muscle degeneration does not affect all the muscles equally. In the studied ASD population, lumbar spine and hip extensor were the groups most affected by muscular degeneration, and muscle volume ratios between flexors and extensors were greatest in the spine group.

ACKNOWLEDGMENTS

Authors thank Dr. Prodromos Parasoglou for help in constructing the fat phantom.

COMMENTS

Background

In adult spinal deformity, recent research has highlighted the critical role of sagittal spino-pelvic alignment in patient-reported pain and function. However these patients are mostly analyzed by skeletal parameters obtained with radiographies, with only a minor consideration on the muscular system which limits the understanding of the pathology.

Research frontiers

Numerous methods have been directed towards analyzing muscular system. However difficulties arise in representing inter-muscle and inter-subject variability as well as obtaining a reliable evaluation of muscular volume and fat infiltration.

Innovations and breakthroughs

Combining Dixon magnetic resonance imaging (MRI) acquisitions and 3D muscular reconstructions, muscular volume and fat infiltration have been obtained for the main functional groups of muscles associated with sagittal posture in the setting of adult spinal deformity. The results have demonstrated that mechanisms of fat infiltration are not similar among the muscle groups for this population. Moreover degeneration mostly impacted the spinal and hip extensors, key muscles in opposition with the anterior sagittal malalignment.

Applications

The results suggest the interest of a complete characterization of the muscular system (including the quantification of the fat infiltration) in the evaluation of patients with spinal deformities.

Terminology

Adult spinal deformity refers to abnormal curvatures of the spine in patients who have completed their growth. Dixon MRI allows the separation of fat and water content and so the calculation of fat infiltration within each muscle.

Peer-review

This manuscript describes an observational study of volume loss and fat infiltration of muscles associated with sagittal posture in patients with adult spinal deformity.

REFERENCES

1 **Lafage V**, Schwab F, Patel A, Hawkinson N, Farcy JP. Pelvic tilt and truncal inclination: two key radiographic parameters in the setting of adults with spinal deformity. *Spine* (Phila Pa 1976) 2009; **34**: E599-E606 [PMID: 19644319 DOI: 10.1097/BRS.0b013e3181aad219]

2 **Schwab F**, Lafage V, Patel A, Farcy JP. Sagittal plane considerations and the pelvis in the adult patient. *Spine* (Phila Pa 1976) 2009; **34**: 1828-1833 [PMID: 19644334 DOI: 10.1097/BRS.0b013e3181a13c08]

3 **Schwab F**, Ungar B, Blondel B, Buchowski J, Coe J, Deinlein D, DeWald C, Mehdian H, Shaffrey C, Tribus C, Lafage V. Scoliosis Research Society-Schwab adult spinal deformity classification:

a validation study. *Spine* (Phila Pa 1976) 2012; **37**: 1077-1082 [PMID: 22045006 DOI: 10.1097/BRS.0b013e31823e15e2]

4 **Schwab FJ**, Blondel B, Bess S, Hostin R, Shaffrey CI, Smith JS, Boachie-Adjei O, Burton DC, Akbarnia BA, Mundis GM, Ames CP, Kebaish K, Hart RA, Farcy JP, Lafage V. Radiographical spinopelvic parameters and disability in the setting of adult spinal deformity: a prospective multicenter analysis. *Spine* (Phila Pa 1976) 2013; **38**: E803-E812 [PMID: 23722572 DOI: 10.1097/BRS.0b013e318292b7b9]

5 **Kawaguchi Y**, Matsui H, Tsuji H. Back muscle injury after posterior lumbar spine surgery. Part 2: Histologic and histochemical analyses in humans. *Spine* (Phila Pa 1976) 1994; **19**: 2598-2602 [PMID: 7855687]

6 **Kawaguchi Y**, Matsui H, Tsuji H. Back muscle injury after posterior lumbar spine surgery. A histologic and enzymatic analysis. *Spine* (Phila Pa 1976) 1996; **21**: 941-944 [PMID: 8726197]

7 **Weber BR**, Grob D, Dvorák J, Müntener M. Posterior surgical approach to the lumbar spine and its effect on the multifidus muscle. *Spine* (Phila Pa 1976) 1997; **22**: 1765-1772 [PMID: 9259789]

8 **Taylor H**, McGregor AH, Medhi-Zadeh S, Richards S, Kahn N, Zadeh JA, Hughes SP. The impact of self-retaining retractors on the paraspinal muscles during posterior spinal surgery. *Spine* (Phila Pa 1976) 2002; **27**: 2758-2762 [PMID: 12486343 DOI: 10.1097/01.BRS.0000035728.24284.6D]

9 **Flicker PL**, Fleckenstein JL, Ferry K, Payne J, Ward C, Mayer T, Parkey RW, Peshock RM. Lumbar muscle usage in chronic low back pain. Magnetic resonance image evaluation. *Spine* (Phila Pa 1976) 1993; **18**: 582-586 [PMID: 8484149]

10 **Gejo R**, Matsui H, Kawaguchi Y, Ishihara H, Tsuji H. Serial changes in trunk muscle performance after posterior lumbar surgery. *Spine* (Phila Pa 1976) 1999; **24**: 1023-1028 [PMID: 10332796]

11 **Kim DY**, Lee SH, Chung SK, Lee HY. Comparison of multifidus muscle atrophy and trunk extension muscle strength: percutaneous versus open pedicle screw fixation. *Spine* (Phila Pa 1976) 2005; **30**: 123-129 [PMID: 15626992]

12 **Lee JC**, Cha JG, Kim Y, Kim YI, Shin BJ. Quantitative analysis of back muscle degeneration in the patients with the degenerative lumbar flat back using a digital image analysis: comparison with the normal controls. *Spine* (Phila Pa 1976) 2008; **33**: 318-325 [PMID: 18303466 DOI: 10.1097/BRS.0b013e318162458f]

13 **Humphrey AR**, Nargol AV, Jones AP, Ratcliffe AA, Greenough CG. The value of electromyography of the lumbar paraspinal muscles in discriminating between chronic-low-back-pain sufferers and normal subjects. *Eur Spine J* 2005; **14**: 175-184 [PMID: 15549487 DOI: 10.1007/s00586-004-0792-3]

14 **Mooney V**, Gulick J, Perlman M, Levy D, Pozos R, Leggett S, Resnick D. Relationships between myoelectric activity, strength, and MRI of lumbar extensor muscles in back pain patients and normal subjects. *J Spinal Disord* 1997; **10**: 348-356 [PMID: 9278921]

15 **Mayer TG**, Vanharanta H, Gatchel RJ, Mooney V, Barnes D, Judge L, Smith S, Terry A. Comparison of CT scan muscle measurements and isokinetic trunk strength in postoperative patients. *Spine* (Phila Pa 1976) 1989; **14**: 33-36 [PMID: 2913665]

16 **Danneels LA**, Vanderstraeten GG, Cambier DC, Witvrouw EE, De Cuyper HJ. CT imaging of trunk muscles in chronic low back pain patients and healthy control subjects. *Eur Spine J* 2000; **9**: 266-272 [PMID: 11261613]

17 **Hultman G**, Nordin M, Saraste H, Ohlsèn H. Body composition, endurance, strength, cross-sectional area, and density of MM erector spinae in men with and without low back pain. *J Spinal Disord* 1993; **6**: 114-123 [PMID: 8504222]

18 **Storheim K**, Holm I, Gunderson R, Brox JI, Bø K. The effect of comprehensive group training on cross-sectional area, density, and strength of paraspinal muscles in patients sick-listed for subacute low back pain. *J Spinal Disord Tech* 2003; **16**: 271-279 [PMID: 12792342]

19 **Barker KL**, Shamley DR, Jackson D. Changes in the cross-sectional area of multifidus and psoas in patients with unilateral back pain: the relationship to pain and disability. *Spine* (Phila Pa 1976) 2004; **29**: E515-E519 [PMID: 15543053]

20 **Dangaria TR**, Naesh O. Changes in cross-sectional area of psoas major muscle in unilateral sciatica caused by disc herniation. *Spine* (Phila Pa 1976) 1998; **23**: 928-931 [PMID: 9580961]

21 **Parkkola R**, Rytökoski U, Kormano M. Magnetic resonance imaging of the discs and trunk muscles in patients with chronic low back pain and healthy control subjects. *Spine* (Phila Pa 1976) 1993; **18**: 830-836 [PMID: 8316880]

22 **Parkkola R**, Kormano M. Lumbar disc and back muscle degeneration on MRI: correlation to age and body mass. *J Spinal Disord* 1992; **5**: 86-92 [PMID: 1571617]

23 **Valentin S**, Licka T, Elliott J. Age and side-related morphometric MRI evaluation of trunk muscles in people without back pain. *Man Ther* 2015; **20**: 90-95 [PMID: 25085813 DOI: 10.1016/j.math.2014.07.007]

24 **Savage RA**, Millerchip R, Whitehouse GH, Edwards RH. Lumbar muscularity and its relationship with age, occupation and low back pain. *Eur J Appl Physiol Occup Physiol* 1991; **63**: 265-268 [PMID: 1836992]

25 **Peltonen JE**, Taimela S, Erkintalo M, Salminen JJ, Oksanen A, Kujala UM. Back extensor and psoas muscle cross-sectional area, prior physical training, and trunk muscle strength--a longitudinal study in adolescent girls. *Eur J Appl Physiol Occup Physiol* 1998; **77**: 66-71 [PMID: 9459523 DOI: 10.1007/s004210050301]

26 **Gille O**, Jolivet E, Dousset V, Degrise C, Obeid I, Vital JM, Skalli W. Erector spinae muscle changes on magnetic resonance imaging following lumbar surgery through a posterior approach. *Spine* (Phila Pa 1976) 2007; **32**: 1236-1241 [PMID: 17495782 DOI: 10.1097/BRS.0b013e31805471fe]

27 **Airaksinen O**, Herno A, Kaukanen E, Saari T, Sihvonen T, Suomalainen O. Density of lumbar muscles 4 years after decompressive spinal surgery. *Eur Spine J* 1996; **5**: 193-197 [PMID: 8831123]

28 **Elliott JM**, Walton DM, Rademaker A, Parrish TB. Quantification of cervical spine muscle fat: a comparison between T1-weighted and multi-echo gradient echo imaging using a variable projection algorithm (VARPRO). *BMC Med Imaging* 2013; **13**: 30 [PMID: 24020963 DOI: 10.1186/1471-2342-13-30]

29 **Tracy BL**, Ivey FM, Jeffrey Metter E, Fleg JL, Siegel EL, Hurley BF. A more efficient magnetic resonance imaging-based strategy for measuring quadriceps muscle volume. *Med Sci Sports Exerc* 2003; **35**: 425-433 [PMID: 12618571 DOI: 10.1249/01.MSS.0000053722.53302.D6]

30 **Jolivet E**. Modélisation biomécanique de la hanche dans le risque de fracture du fémur proximal [Internet]. 2007. Available from: URL: https://pastel.archives-ouvertes.fr/pastel-00003206

31 **Jolivet E**, Dion E, Rouch P, Dubois G, Charrier R, Payan C, Skalli W. Skeletal muscle segmentation from MRI dataset using a model-based approach. *Comput Methods Biomech Biomed Eng Imaging Vis* 2014; **2**: 138-145 [DOI: 10.1080/21681163.2013.855146]

32 **Jolivet E**, Daguet E, Pomero V, Bonneau D, Laredo JD, Skalli W. Volumic patient-specific reconstruction of muscular system based on a reduced dataset of medical images. *Comput Methods Biomech Biomed Engin* 2008; **11**: 281-290 [PMID: 18568825 DOI: 10.1080/10255840801959479]

33 **Südhoff I**, de Guise JA, Nordez A, Jolivet E, Bonneau D, Khoury V, Skalli W. 3D-patient-specific geometry of the muscles involved in knee motion from selected MRI images. *Med Biol Eng Comput* 2009; **47**: 579-587 [PMID: 19277749 DOI: 10.1007/s11517-009-0466-8]

34 **Moal B**, Raya JG, Jolivet E, Schwab FJ, Blondel B, Lafage V, Skalli W. Validation of 3D spino-pelvic muscle reconstructions based on dedicated MRI sequences for fat-water quantification. *IRBM* [Internet] 2014; **33**: 0-9 [DOI: 10.1016/j.irbm.2013.12.011]

35 **Dixon WT**. Simple proton spectroscopic imaging. *Radiology* 1984; **153**: 189-194 [PMID: 6089263 DOI: 10.1148/radiology.153.1.6089263]

36 **Gaeta M**, Messina S, Mileto A, Vita GL, Ascenti G, Vinci S, Bottari A, Vita G, Settineri N, Bruschetta D, Racchiusa S, Minutoli F. Muscle fat-fraction and mapping in Duchenne muscular dystrophy: evaluation of disease distribution and correlation with clinical assessments. Preliminary experience. *Skeletal Radiol* 2012; **41**: 955-961 [PMID: 22069033 DOI: 10.1007/s00256-011-1301-5]

37 **Ragan DK**, Bankson JA. Two-point Dixon technique provides robust fat suppression for multi-mouse imaging. *J Magn Reson Imaging* 2010; **31**: 510-514 [PMID: 20099366 DOI: 10.1002/jmri.22060]

38 **Cassidy FH**, Yokoo T, Aganovic L, Hanna RF, Bydder M, Middleton MS, Hamilton G, Chavez AD, Schwimmer JB, Sirlin CB. Fatty liver disease: MR imaging techniques for the detection and quantification of liver steatosis. *Radiographics* 2009; **29**: 231-260 [PMID: 19168847]

39 **Shen W**, Gong X, Weiss J, Jin Y. Comparison among T1-weighted magnetic resonance imaging, modified dixon method, and magnetic resonance spectroscopy in measuring bone marrow fat. *J Obes* 2013; **2013**: 298675 [PMID: 23606951 DOI: 10.1155/2013/298675]

40 **Kim H**, Taksali SE, Dufour S, Befroy D, Goodman TR, Petersen KF, Shulman GI, Caprio S, Constable RT. Comparative MR study of hepatic fat quantification using single-voxel proton spectroscopy, two-point dixon and three-point IDEAL. *Magn Reson Med* 2008; **59**: 521-527 [PMID: 18306404 DOI: 10.1002/mrm.21561]

41 **Cruz-Jentoft AJ**, Baeyens JP, Bauer JM, Boirie Y, Cederholm T, Landi F, Martin FC, Michel JP, Rolland Y, Schneider SM, Topinková E, Vandewoude M, Zamboni M. Sarcopenia: European consensus on definition and diagnosis: Report of the European Working Group on Sarcopenia in Older People. *Age Ageing* 2010; **39**: 412-423 [PMID: 20392703 DOI: 10.1093/ageing/afq034]

42 **Song MY**, Ruts E, Kim J, Janumala I, Heymsfield S, Gallagher D. Sarcopenia and increased adipose tissue infiltration of muscle in elderly African American women. *Am J Clin Nutr* 2004; **79**: 874-880 [PMID: 15113728]

43 **Horton WC**, Brown CW, Bridwell KH, Glassman SD, Suk SI, Cha CW. Is there an optimal patient stance for obtaining a lateral 36" radiograph? A critical comparison of three techniques. *Spine* (Phila Pa 1976) 2005; **30**: 427-433 [PMID: 15706340]

44 **Champain S**, Benchikh K, Nogier A, Mazel C, Guise JD, Skalli W. Validation of new clinical quantitative analysis software applicable in spine orthopaedic studies. *Eur Spine J* 2006; **15**: 982-991 [PMID: 15965708 DOI: 10.1007/s00586-005-0927-1]

45 **Rillardon L**, Levassor N, Guigui P, Wodecki P, Cardinne L, Templier A, Skalli W. [Validation of a tool to measure pelvic and spinal parameters of sagittal balance]. *Rev Chir Orthop Reparatrice Appar Mot* 2003; **89**: 218-227 [PMID: 12844045]

46 **Terran J**, Schwab F, Shaffrey CI, Smith JS, Devos P, Ames CP, Fu KM, Burton D, Hostin R, Klineberg E, Gupta M, Deviren V, Mundis G, Hart R, Bess S, Lafage V. The SRS-Schwab adult spinal deformity classification: assessment and clinical correlations based on a prospective operative and nonoperative cohort. *Neurosurgery* 2013; **73**: 559-568 [PMID: 23756751 DOI: 10.1227/NEU.0000000000000012]

47 **Blondel B**, Schwab F, Ungar B, Smith J, Bridwell K, Glassman S, Shaffrey C, Farcy JP, Lafage V. Impact of magnitude and percentage of global sagittal plane correction on health-related quality of life at 2-years follow-up. *Neurosurgery* 2012; **71**: 341-348; discussion 348 [PMID: 22596038 DOI: 10.1227/NEU.0b013e31825d20c0]

48 **Glassman SD**, Bridwell K, Dimar JR, Horton W, Berven S, Schwab F. The impact of positive sagittal balance in adult spinal deformity. *Spine* (Phila Pa 1976) 2005; **30**: 2024-2029 [PMID: 16166889]

49 **Smith JS**, Klineberg E, Schwab F, Shaffrey CI, Moal B, Ames CP, Hostin R, Fu KM, Burton D, Akbarnia B, Gupta M, Hart R, Bess S, Lafage V. Change in classification grade by the SRS-Schwab Adult Spinal Deformity Classification predicts impact on health-related quality of life measures: prospective analysis of operative and nonoperative treatment. *Spine* (Phila Pa 1976) 2013; **38**: 1663-1671 [PMID: 23759814 DOI: 10.1097/BRS.0b013e31829ec563]

50 **Fischer MA**, Nanz D, Shimakawa A, Schirmer T, Guggenberger R, Chhabra A, Carrino JA, Andreisek G. Quantification of muscle fat in patients with low back pain: comparison of multi-echo MR imaging with single-voxel MR spectroscopy. *Radiology* 2013; **266**: 555-563 [PMID: 23143025 DOI: 10.1148/radiol.12120399]

51 **Kovanlikaya A**, Guclu C, Desai C, Becerra R, Gilsanz V. Fat quantification using three-point dixon technique: in vitro validation. *Acad Radiol* 2005; **12**: 636-639 [PMID: 15866138 DOI: 10.1016/j.acra.2005.01.019]

52 **de Bazelaire CM**, Duhamel GD, Rofsky NM, Alsop DC. MR imaging relaxation times of abdominal and pelvic tissues measured in vivo at 3.0 T: preliminary results. *Radiology* 2004; **230**: 652-659 [PMID: 14990831 DOI: 10.1148/radiol.2303021331]